

Large-scale structure of a nation-wide production network

Yoshi Fujiwara¹ and Hideaki Aoyama²

¹*NiCT/ATR CIS, Applied Network Science Lab, Kyoto 619-0288, Japan*

²*Department of Physics, Kyoto University, Kyoto 606-8501, Japan*

Production in an economy is a set of firms' activities as suppliers and customers; a firm buys goods from other firms, puts value added and sells products to others in a giant network of production. Empirical study is lacking despite the fact that the structure of the production network is important to understand and make models for many aspects of dynamics in economy. We study a nation-wide production network comprising a million firms and millions of supplier-customer links by using recent statistical methods developed in physics. We show in the empirical analysis scale-free degree distribution, disassortativity, correlation of degree to firm-size, and community structure having sectoral and regional modules. Since suppliers usually provide credit to their customers, who supply it to theirs in turn, each link is actually a creditor-debtor relationship. We also study chains of failures or bankruptcies that take place along those links in the network, and corresponding avalanche-size distribution.

I. INTRODUCTION

The physics community has recently witnessed considerable development of statistical methods for quantifying large networks, including biology, information, technology, economics and society [1–3]. The development enables one to quantify statistical features, modular and heterogeneous structures of large networks that are not amenable even to visualization.

Production network in economics refers to a line of economic activities in which firms buy intermediate goods from “upstream” firms, put value added on them, and sell the goods to “downstream” firms. Net sum of value added in the whole network is basically the net total production in a nation, that is, gross domestic product (GDP).

Consider a ship manufacturer, for example. The manufacturer buys a number of intermediate goods including steel materials, mechanical and electronic devices, etc. and produces ships. The firm puts value added on the products in each process of production. In the upstream side of the ship manufacturer, a processed steel manufacturer could be present, which in turn buys intermediate goods such as raw steel and fabricating machines. The steel manufacturer may supply its products to car manufactures as well. Similarly in the downstream side, including retail and wholesale firms.

The entire line of these processes of putting value added in turn, therefore, forms a giant web of production ranging from upstream to downstream, ultimately down to consumers. Each firm needs labor and financing in addition to intermediate goods, and utilizes these inputs to produce outputs in *anticipation* for return of profits. Thus, a real economy has its driving force in production, and is fueled by labor and financing.

There are studies based on theoretical models of production networks, notably in overlapping communities between economists and physicists. They include inventory dynamics [4–6] (see also [7]), suppliers/customers dynamics [8], and credit-chain model [9–11]. These promising works are, unfortunately, not based on any

empirical study on the structure of production networks. While economic networks of inter-bank [12–14], banks-firms [15] financing relations, and inter-firm ownerships [16, 17] are studied based on recent empirical data (see [18] and references therein), there exists a gap to be filled in the study of inter-firm credit and supplier-customer relations. So it is highly desirable to investigate the structure of production network on a nation-wide scale to develop insightful models, but such a study has been considered a formidable task so far.

The present paper precisely performs such an empirical study of the large-scale structure of a production network that comprises most firms in a nation as nodes, and supplier-customer relations as links. We will find that the network is not regular nor random, but possesses scale-free degree distribution, disassortativity, as well as other statistical properties, and structural modules that depend on industrial sectors and geographical regions with highly varying modular sizes.

The structural heterogeneity would have many important consequences in *dynamics* on a production network. For example, demand by firms and consumers downstream will propagate upstream; when foreign countries increase demand for ships, it will result in a growing output of ship manufacturers, which possibly stimulate production of processed steel, raw metals, related machines etc. in upstream firms. This propagation will not take place homogeneously but heterogeneously.

Conversely, decreasing demand also causes a chain reaction. An individual firm's profit is equal to sales *minus* costs. It may use factors of production in anticipation of profit, but always faces uncertainty in ex-post demand, labor and financial costs, price change of intermediate goods, and so forth. Only *a posteriori*, profits are determined through the interaction of firms in the production network. Once a firm goes into a state of financial insolvency or bankruptcy, its upstream firms have its balance-sheets deteriorated by losing fractional profits, and may eventually go into bankruptcy. We will show that such a chain of failure is by no means negligible, due to the network structure, and so that this has a considerable

effect at macroeconomic activity.

In Section II, we describe how nodes and links are surveyed and recorded in our dataset of a production network, in addition to another dataset of an exhaustive list of bankruptcies occurred in the network over a certain period of time. In Section III, we study the structure of the production network by employing statistical methods in [1–3]. In Section IV, we extract community structure in the network. In Section V, we examine the chains of bankruptcies with a focus on avalanche-size distribution. After a brief discussion in Section VI, we conclude in Section VII.

II. SUPPLIER-CUSTOMER LINKS AND BANKRUPTCY DATA

Let us say that a directional link is present as $A \rightarrow B$ in a production network, where firm A is a supplier to another firm B , or equivalently, B is a customer of A . While it is difficult to record every transaction of supply and purchase among firms, it is also pointless to have a record that a firm buys a pencil from another. Necessary for our study are data of links such that the relation $A \rightarrow B$ is crucial for the activity of one or both A and B . If at least one of the firms at either end of a link nominates the other firm as most important suppliers or customers, then the link should be listed.

Our dataset for supplier-customer links is based on this idea. Tokyo Shoko Research, Inc., one of the leading credit research agencies in Japan, regularly gathers credit information on most of active firms through investigation of financial statements and corporate documents, and by hearing-based survey at branch offices located across the nation. Financial and credit information of individual firms are compiled in commercially available databases. The credit information of individual firm includes its suppliers and customers, up to 24 companies for each, that are considered to be most crucial for its business activities. We assume that the links playing important roles in the production network are recorded at either end of each link as we describe above, while we should understand that it is possible to drop relatively unimportant links from the data. Although amounts of transactions provide information of weights on links, that is of relative importance regarding suppliers and customers, such data are only partially available at the moment. We simply ignore the weights in this paper. It is also remarked that the financial sector is under-represented in the database as those financial companies' links are not included.

We have a snapshot of production networks compiled in September 2006. In the data, the number of firms is roughly a million, and the number of directional links is more than four million (see Section III). The set of nodes in the network covers essentially most of the domestic firms that are active in the sense that their credit information is required. Attached to each firm is financial information of firm-size, which is measured as sales, profit,

TABLE I: Classification of industrial sectors. Third column shows numbers of major-groups/groups/industries classified in each division. Fourth column are fractional numbers of firms in the divisions according to primary industry of each firm in the dataset of September 2006.

divisions ^a	#class. ^a	#firms(%)
A agriculture	1/4/20	0.53
B forestry	1/5/9	0.05
C fisheries	2/4/17	0.11
D mining	1/6/30	0.18
E construction	3/20/49	29.92
F manufacturing	24/150/563	17.69
G electricity/gas/heat/water	4/6/12	0.06
H information/communications	5/15/29	2.42
I transport	7/24/46	3.54
J wholesale/retail trade	12/44/150	29.07
K finance/insurance	7/19/68	0.65
L real estate	2/6/10	2.61
M food establishments	3/12/18	1.46
N medical/health care/welfare	3/15/37	1.03
O education/learning support	2/12/33	0.36
P compound services ^b	2/4/8	0.64
Q services ^c	15/68/164	9.45
R government ^c	2/5/5	0.18
S unable to classify	1/1/1	0.03
Total	97/420/1,269	99.98

^aJapan Standard Industrial Classification, Rev. 11, March 2002: <http://www.stat.go.jp/english/index/seido/sangyo/index.htm>

^bGovernment-affiliated postal services, and agriculture, forestry, fisheries and business cooperative associations.

^cNot elsewhere classified.

number of employees and their growth, major and minor classification into industrial sectors, details of products, the firm's banks, principal shareholders, and miscellaneous information including geographical location. In particular, the industrial sectors are classified into more than 1,200 industries and are categorized hierarchically into 19 divisions, 97 major groups and more than 400 minor groups (see Table I). For example, the manufacturing sector (F) is classified into 24 major groups as tabulated in Table II. Each firm has industry classification according to the sector it belongs to as primary (also secondary and tertiary, if any) industry.

In addition, we use a database that records “dead” firms, namely business failure or bankruptcy. This dataset is an exhaustive list of bankrupted firms since October 2006 for one year, corresponding to the snapshot of the network. The data is exhaustive in the sense that any bankrupted firm with a total amount of debt exceeding 10 million yen (roughly 70 thousand euro or 100 thousand US dollar) is listed therein. Each record includes the date of failure, the total amount of debt when bankrupted and categorized causes of bankruptcy. The dataset has high quality and its statistical tabulation is employed by the Statistics Bureau of government for an official statistics. In the production network, 0.5% to 1% of nodes exit in a year due to failure (see Section V). Thus, by combining

TABLE II: 24 major groups of the manufacturing sector (F).

id	major group	#firms(%)
09	foods	10.15
10	beverages, tobacco and feed	1.95
11	textile mill products, except apparel/related	3.08
12	apparel and related finished products	5.00
13	lumber and wood products, except furniture	3.57
14	furniture and fixtures	2.44
15	pulp, paper and paper products	2.90
16	printing and allied industries	6.51
17	chemical and allied products	3.28
18	petroleum and coal products	0.29
19	plastic products, except otherwise classified	4.98
20	rubber products	1.10
21	leather tanning, leather/fur products	0.83
22	ceramic, stone and clay products	5.09
23	iron and steel	1.97
24	non-ferrous metals and products	1.35
25	fabricated metal products	12.30
26	general machinery	13.83
27	electrical machinery, equipment and supplies	5.08
28	information and communication electronics	1.33
29	electronic parts and devices	2.57
30	transportation equipment	3.19
31	precision instruments and machinery	2.06
32	miscellaneous manufacturing industries	5.14

the two datasets of supplier-customer links and actual failures, one has an opportunity to do an empirical study of the dynamics of failure on the production network. And this point differs from the previous studies on the Japanese production network including [19, 20].

III. STRUCTURE OF PRODUCTION NETWORK

A. Global connectivity

The production network as a directed graph is not unidirectional from upstream to downstream, but is highly entangled depending on the products and services that each firm produces. Let us first examine the global connectivity by using a similar graph-theoretical method as was performed in the study of the hyperlink structure of the world-wide web [21]. The following numbers are for the dataset of September 2006, which contains 1,019,854 firms as nodes of the network excluding all the bankrupted firms before the month.

From a directed graph, one can obtain an undirected graph by simply ignoring the direction of links. A weakly connected component of the directed graph refers to a connected component in the undirected counterpart. The production network has a giant weakly connected component (GWCC) comprised of 99.0% (1,009,597 nodes) of the whole. The rest are disconnected components, all of which are smaller than 12 in size.

A strongly connected component (SCC) in a directed

graph is a set of nodes such that for any pair of nodes u and v in the set there is a directed path from u to v . There exists a giant SCC having the size of 45.8% of the GWCC (462,563 nodes). Calling it GSCC, the GWCC turns out to be decomposed into mutually disjoint parts as $\text{GWCC} = \text{GSCC} + \text{IN} + \text{OUT} + \text{TE}$, where IN is the set of non-GSCC nodes, from which one can reach a node (so all the nodes) in the GSCC. Symmetrically, OUT is the set of non-GSCC nodes, to which one can go from any node in the SCC. And TE is the rest of the GWCC, called tendrils, which consists of nodes that have no access to the GSCC and are not reachable from it. Hanging off IN and OUT are tendrils containing nodes that are reachable from portions of IN, or that can reach to portions of OUT, without passing through the SCC. See Figure 6 in [2] understanding their definitions for giant GIN and GOUT as $\text{GIN} = \text{IN} + \text{GSCC}$ and $\text{GOUT} = \text{OUT} + \text{GSCC}$. The IN, OUT and TE are composed of 18.0% (182,018), 32.1% (324,569) and 4.0% (40,447) nodes, respectively, in the GWCC.

By comparing the abundance of industrial divisions in each of these giant components, we observe that in the portion of IN the numbers of firms in the sectors of real estate (L), forestry (B), information and communications (H) are larger when compared with the corresponding sectors in the SCC. In the portion of OUT more abundant are medical, health care and welfare (N), food establishments (M), education (O). This fact is reasonable, because these industries are located either in the upstream or in the downstream. Nevertheless, all industries are basically embedded in the SCC with entanglement. We shall study community structure in Section IV.

The diameter of a graph is the maximum length for all ordered pairs (u, v) of the shortest path from u to v . The average distance is the average length for all those pairs (u, v) . We found that the average distance is 4.59 while the diameter is 22.

B. Degree distribution

In the rest of this paper, we focus on the GWCC ignoring small disconnected components. Denoting the numbers of nodes and links by N and M respectively, they are for the GWCC

$$N = 1,009,597, \quad (1)$$

$$M = 4,041,442. \quad (2)$$

A firm has suppliers for and customers of it, whose numbers are in-degree and out-degree, respectively, according to our definition of link direction. We show that both have a long-tail distribution. Denoting the degree distribution by $P(k)$, cumulative distribution is written as $P_{>}(k) = \sum_{k'=k}^{\infty} P(k')$. We plot the cumulative distributions for in and out-degrees in Fig. 1.

Both for in-degree and out-degrees of a firm, the distribution has a heavy tail that can be characterized by a

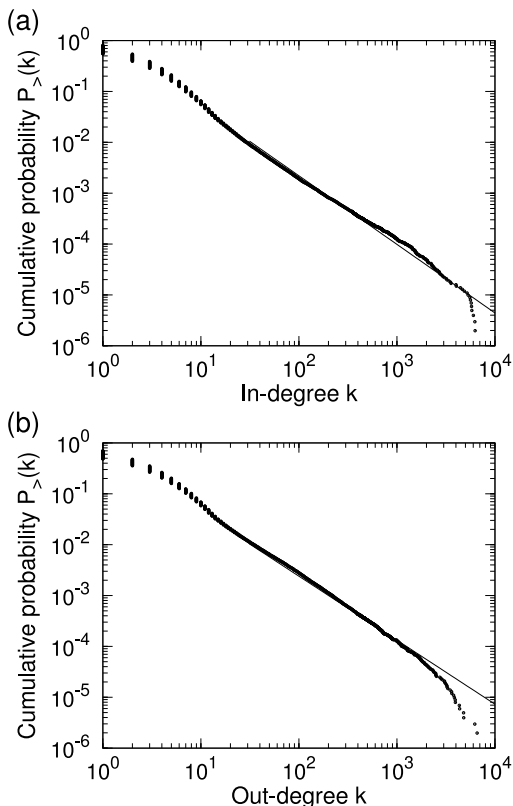


FIG. 1: (a) Cumulative distribution for in-degree (number of suppliers). A power-law distribution $P_{>}(k) \propto k^{-\mu}$ is fitted by MLE with $\mu = 1.35 \pm 0.02$ (a solid line). (b) Same for out-degree (number of customers). The line is for $\mu = 1.26 \pm 0.02$.

power-law $P_{>}(k) \propto k^{-\mu}$. We estimated the exponent μ by maximum likelihood (MLE), *i.e.* the Hill's estimate [22], in a tail-region $k > k_*$. In Fig. 1, the estimates are shown for $k_* = 40$, namely $\mu = 1.35 \pm 0.02$ for in-degree and $\mu = 1.26 \pm 0.02$ for out-degree, by solid lines. Here the errors correspond to 1.96σ (99% significance level) of the estimated standard errors σ .

The first two moments of in/out-degree are

$$\langle k_{\text{in}} \rangle \equiv \langle k_{\text{out}} \rangle = 4.003, \quad (3)$$

$$\langle k_{\text{in}}^2 \rangle = 1.041 \times 10^3, \quad \langle k_{\text{out}}^2 \rangle = 1.036 \times 10^3. \quad (4)$$

For the undirected graph, we have

$$\langle k \rangle = 2M/N = 8.006, \quad (5)$$

$$\langle k^2 \rangle = 3.070 \times 10^3. \quad (6)$$

Firms with largest in-degrees belong to the sectors of manufacturing and construction among others, including heavy industry, electrical machinery (e.g. Hitachi, Mitsubishi, Panasonic, Toshiba), automobiles (Toyota, Nissan, Honda), metal production, and so on. Large construction companies are also included. Firms with the largest out-degrees are worldwide traders, distributors of construction-related materials, metals, petroleum, mechanical and electrical instruments, and general whole-

sale companies, as well as the manufacturing firms mentioned for in-degrees.

C. Correlation to firm-size

The number of suppliers/customers of a firm depends obviously on firm-size, an important attribute. A large firm likely possesses numerous suppliers to buy various intermediate goods; similarly it has a number of customers to sell its products to so that it has the large size. Firm-size can be measured in different ways, basically by *stock* variables (total-asset, number of employees, etc.) or *flow* variables (sales, profits, etc.).

The firm-size, however measured, obeys a power-law, being well known as a Zipf's law. For the nodes in the network, we examined financial data (availability exceeds 70% presumably missing only extremely small firms). The cumulative distribution for the sales of those nodes (0.73 million) is shown in Fig. 2 (a). The Zipf's law, $P_{>}(x) \propto x^{-\alpha}$, is obvious for sales x . The exponent is close to unity, $\alpha = 0.96 \pm 0.02$ by MLE estimated for $x > 10^4$ million yen.

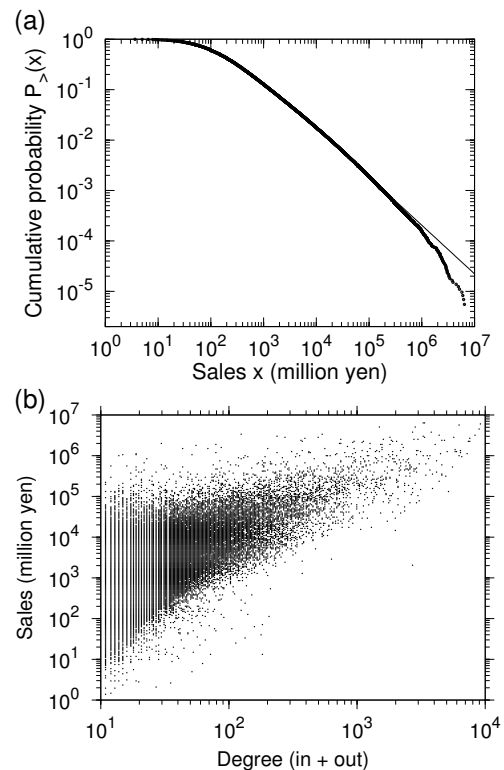


FIG. 2: (a) Cumulative distribution for firm-size measured by sales. A power-law distribution $P_{>}(x) \propto x^{-\alpha}$ is fitted by MLE with $\alpha = 0.96 \pm 0.02$ (a solid line). (b) Scatter-plot for degree (total) and sales.

Fig. 2 (b) depicts a scatter-plot for total degree and sales. Correlation between the firm's degree and size

is positive. The statistical significance can be quantified by non-parametric statistics, such as Kendall's rank correlation, τ (see [23]). For the data, $\tau = 0.391$ (p -value $< 10^{-7}$), which shows a significant positive correlation between the degree and firm-size. We used different quantities for firm-size, such as profits and the number of employees, and obtained very similar results. In addition, when considering either of in- or out-degree, we can observe that each has a positive correlation with firm-size.

D. Transitivity

Unlike many social networks, the supplier of a firm's supplier is not likely also to be the firm's supplier, and similarly for customer, because such a process of production is redundant for most cases. Transitivity means how high the number of triangles is present in the network (see the review [3]). Here we regard the network as an undirected graph.

Global clustering coefficient is defined by $C_g = (3 \times \text{number of triangles}) / (\text{number of connected triples})$, where a connected triple means a pair of nodes that are connected to another node. C_g is the mean probability that two firms who have a common supplier/customer are also suppliers/customers of each other. The undirected graph of our dataset yields

$$C_g = 1.87 \times 10^{-3} = 0.187\% . \quad (7)$$

To compare this value with that for a class of random graphs having a same degree sequence but randomly rewired links, we use the expected value of global clustering coefficient given by [24]

$$C_g = \frac{\langle k \rangle}{N} \left[\frac{\langle k^2 \rangle - \langle k \rangle^2}{\langle k \rangle^2} \right]^2 . \quad (8)$$

Putting the values (5), (6) and (1) into (8), we have $C_g = 1.81 \times 10^{-2}$. The observed value (7) is, therefore, merely 10% of (8), and shows weaker transitivity than what is expected by chance. This is reasonable because triangular relations, during the selection of suppliers and customers, are suppressed in the formation of them.

The average of local clustering coefficient is, on the other hand, equal to 4.58% for the same dataset.

E. Degree correlation

For each node, the in-degree and out-degree are highly correlated. This is consistent with what we saw in Section III C that each quantity has positive correlation with firm-size.

For each link, to see the assortative mixing with respect to degrees (k_1, k_2) at both end of each link [25], or degree correlation, let us examine the joint distribution for

(k_1, k_2) . Here we ignore the direction of links, but even when taking the possible four combinations of in/out at a directed link, we obtain similar results. To test for the assortativity, we calculate the frequency $F(k_1, k_2)$ that the pair of k_1 and k_2 appears at either end of a link in the network. Then compare it with a same quantity $F_r(k_1, k_2)$ that is obtained in a randomized network with the same degree sequence. We generated 1,000 randomized networks, and quantify as the ratio F/F_r where F_r is the average for the randomizations.

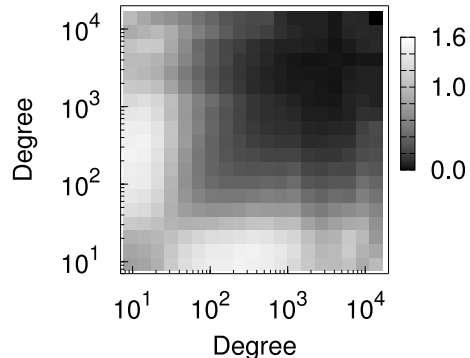


FIG. 3: Joint distribution for degrees (total) at end of each link. The value is the ratio of the actual frequency divided by what is expected by chance in random networks with the same degree sequence as the actual one.

The result is shown in Fig. 3. One can observe that large-degree nodes, large firms, are connected with small-degree nodes, small firms. For the hubs referred to in the end of Section III B, they have a large number of suppliers and customers, but similarly for firms with intermediate-size, displaying disassortativity [25]. This can be quantified by the Pearson correlation coefficient r for (k_1, k_2) . For the data, we have

$$r = -0.0747 \pm 0.0002 , \quad (9)$$

where the error calculated by the method given in [25]. This claims that r is negative with a statistical significance.

IV. COMMUNITY STRUCTURE

The global connectivity examined in Section III A shows that basically all industries are highly entangled with each other within the weakly or strongly connected component. Yet the connectivity alone does not tell how dense or sparse the stream of production is distributed depending on industrial or geographical groups. Detection of community structure is to find how nodes cluster into tightly-knit groups with high density in intra-groups and with lower connectivity in inter-groups.

We focus, in this section, on the manufacturing sector with 0.12 million firms, in order to understand the sector's modular structure by excluding other dominant

TABLE III: Communities extracted for the subgraph composed of manufacturing firms as nodes (about 0.12 million). Modularity optimization was recursively done for largest communities to obtain the sub-communities, ten of which are shown here. In each of them are shown ten firms with largest degrees are listed with names, major groups (primary/secondary/tertiary, if any in this order) of industrial sectors (see Table II), and sub-community sizes.

no.	annotation	firms (major groups; primary/secondary/tertiary), ...	[community-size]
01	heavy industry	Mitsubishi Heavy Industries (30/26), Kawasaki Heavy Industries (26/30), Kobe Steel (23/25), Ishikawajima-harima Heavy Industries (30/26), Sumitomo Heavy Industries (26), Nippon Steel (23), Kubota Industries (30/27/23), Mitsui Engineering and Shipbuilding (30), Hitachi Zosen Shipbuilding (26), Sumitomo Metal Industries (23), ...	[7,447]
02	foods	Itoham Foods (09), Prima Meat Packers (09), Yamazaki Baking (09), Nisshin Seifun Flour (09), Maruha Nichiro Foods (09), Nippon Flour Mills (09), Q.P. Foods (09), Nihon Shokken Foods (09), Toyo Suisan Foods (09), Ichiban-foods (09), ...	[7,115]
03	transportation equipment	Honda (30/27), Nissan (30), Toyota Motor (30), Aisin (25/30/27), Mitsubishi Motors (30), Denso (30/27), Fuji Heavy Industries (30), Toyota Industries (30/26), Suzuki Motor (30), Isuzu Motors (30), ...	[5,769]
04	construction material	Sumitomo Osaka Cement (22), Air-Water Industrial Gas (17/18), Kyowa Concrete (22), Hokukon Concrete (22), Marukin Steel Materials (23), Mitsubishi Construction Materials (25/22), Hinode Steel/Manhole (23/22), Nihon Kogyo Industrial (22/13), Lafarge Aso Cement (22), Maeta Concrete (22), ...	[2,644]
05	pulp/paper	Oji Paper (15), Rengo Paper (15), Nippon Paper (15), Oji Chiyoda Container (15), Tomoku Container (15), Morishigyo Paper (15), Settsu Carton (15), Morishigyo Paper Sales (15), Crown Package (15), Yamatoshiki Paper (15/19), ...	[3,697]
06	electronics(a)	Hitachi (28/29/27), Fujitsu (32/28), NEC (28/29), TDK (27/29), Oki Electric (28/29), Hitachi High-Technologies (31/26), Rohm Semi-conductors (29), Murata Electronics (27), IBM Japan (28), Japan Radio Communication Equipment (28/27), ...	[3,082]
07	electronics(b)	Matsushita (Panasonic) (27/31), Sharp (29/27/28), Sanyo (27/25), Panasonic Shikoku Electronics (29/27/28), Pioneer (27/28), Matsushita Battery (27), Sanyo Tottori (28), Matsushita Refrigeration (27/26), Kenwood (28), CMK Electronic Devices (29), ...	[2,921]
08	electronics(c)	Canon (28/26/31), Seiko Epson (28/29), Omron (27), Nikon (31/26), Ricoh (26/28), Fujinon Optics (31), Hoya Optics (31), Casio (26/31/28), Pentax Optics (31/28), Sony EMCS Electronic (27/28), ...	[2,692]
09	electronics(d)	Toshiba (27/28/29), Stanley Electric (27/26), Toshiba Lighting and Technology (27/26/29), Ushio Electric (25/27/26), Hamamatsu Photonics (29/27), Nippon Electric Glass (22), Toshiba Tec (26/27), GS Yuasa Industry (27/29), Iwasaki Electric (27), Topcon Electric (31), ...	[2,320]
10	apparel	Renoun Apparel (12), Onward Kashiyama Apparel (12), MC Knit Apparel (12), World Apparel (12), Sanyo Shokai Apparel (12), Itokin Apparel (12), Fujii Fabrics (11), Sanei-International Apparel (12), YKK Fastening and Accesaries (32), World Apparel (12), ...	[1,567]

sectors including wholesale and retail trade, which obviously have a different role in the stream of production from the core of manufacturing sector.

We use the method of maximizing modularity, introduced by [26] and implemented for large-scale graphs in [27] as a greedy optimization. While considerable studies have been conducted to develop various methods for community extraction, we use the modularity optimization for its clear interpretation in terms of statistical hypothesis (also see [28] for a comparative study). Let e_{ij} be the fraction of edges in the network that connect nodes in group i to those in group j , and let $a_i \equiv \sum_j e_{ij}$, $b_j \equiv \sum_i e_{ij}$. Then modularity Q is defined by

$$Q = \sum_i (e_{ii} - a_i b_i) \quad (10)$$

which is the fraction of edges that fall within groups, minus the expected value of the fraction under the hypothesis that edges fall randomly irrespectively of the community structure. The method is formulated as an optimization problem to find a partition of nodes into mutually disjoint groups such that the corresponding value of Q is maximum.

As shown in [29, 30], however, the method can give undesired grouping, depending on the density of connections and the network size. Especially, large communities can potentially contain sub-communities. Currently, without an established method to avoid this problem of resolution limit (see [31], for example, and also [32]), we shall check the structure of detected communities by constraining modularity optimization on each single community, especially for those with relatively large community-size.

We apply the method of community extraction to the undirected subgraph whose nodes consist of only firms in the manufacturing sector (division F in Table I). The resulting modularity (10) is $Q = 0.566 \pm 0.001$, which indicates strong community structure (the error calculated by the method given in [25]). The number of extracted communities exceeds a thousand, whose sizes range from a few to more than 10,000. From the database of the information on the firms, we found that many of those small communities are each located in same geographical areas forming specialized production flows. An example is a small group of flour-maker, noodle-foods producers, bakeries, and packing/labeling companies in a rural area.

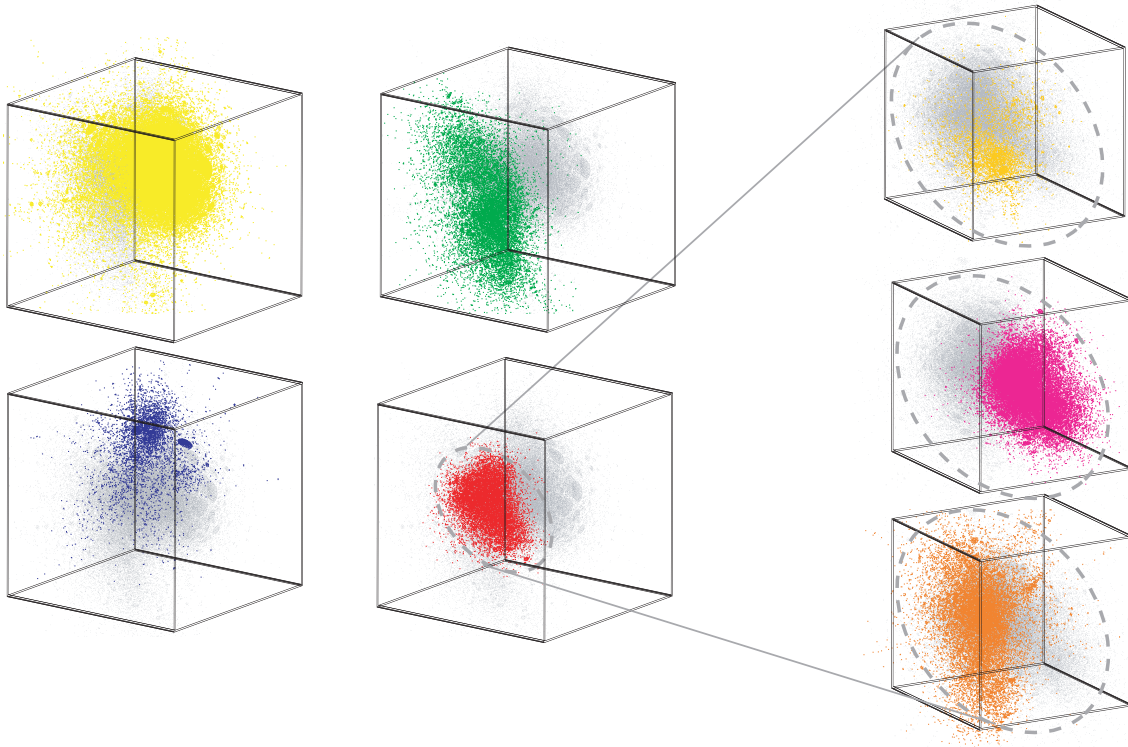


FIG. 4: (Color online) Layout of nodes for firms in the manufacturing sector (F) by a force-directed method. The links are omitted, and different colors are put on the nodes belonging to four largest communities. The community of color red (middle bottom and encircled by a dotted line) is divided into three sub-communities of electronics (a), (b) and (c) given in Table III (enlarged in the right column).

On the other hand, five large communities exceed 10,000 each in size, being possibly subject to the above problem of resolution. After checking the sub-communities in the above mentioned fashion, we obtained the communities as tabulated in Table III. The necessity of this procedure can be clearly seen for the communities of so-annotated “electronics” (a)–(d), which constitute a single community in the first stage of optimization. Each firm is classified into one or more industrial sectors, and the major-group classifications (2 digits; see Table II). Obviously a community contains those firms in closely related industrial sectors. The annotations — heavy industries, foods, transportation equipment, etc. — are made by such observations.

Let us closely examine the modular structure of those large communities. Note that ten firms with the largest degrees (typically largest firm-sizes) are listed in each community. We note that these large firms in a same community do not form a set of nodes that are mutually linked in nearly all possible ways, or a quasi-clique. Rather, with their suppliers and customers, they form a quasi-clique in a corresponding bipartite graph as follows. A supplier-customer link $u \rightarrow v$ for a set of nodes V ($u, v \in V$) can be considered as an edge in a bipartite graph that has exactly two copies of V as V_1 and V_2 ($u \in V_1$ and $v \in V_2$). Those large and competing firms quite often share a set of suppliers to some extent, de-

pending on the industrial sectors, geographical locations and so on.

For example, Honda (v_1), Nissan (v_2) and Toyota (v_3) possibly have a number of suppliers u_i of mechanical parts, electronic devices, chassis and assembling machines, etc., in common. Then the links form a clique or a quasi-clique in the bipartite graph, where most possible links from u_i to v_1, v_2, v_3, \dots are present. This forms a portion in the original graph with a higher density than other portions. By enumerating cliques in the bipartite graph and examining them, we found that this is actually the case for the community (03) in Table III, and similarly for all the other communities therein.

For the case of electronics (a)–(d), those quasi-cliques are further separated into groups. Namely, the suppliers belong to different groups of industrial organization for historical reasons and the so-called *keiretsu*, and/or are located in divided geographical sectors. The sub-communities (a)–(d) can be considered as such separate groups with mutually sparse links. The electronics (b), for instance, are originated and developed in an urban area in western Japan, not in eastern urban area of the Tokyo, being different from group (a).

These interpretations of modular structure should be strengthened by more detailed analysis, especially with a new technique for extraction of communities that are present in multi-scale levels in the hierarchical organiza-

tion of the production of network (see [33, 34] for example), which is to be published elsewhere.

Here, to check the intra-group and inter-group connectivities, we resort to visualization of the entire manufacturing sector by a graph layout based on a physical simulation. The system in the simulation consists of point-particles for nodes and springs for links. The springs obey Hooke's law with a spring constant, and the particles have a Coulomb charge with a same sign, exerting repulsive forces inversely proportional to the square of mutual distances, for nodes to spread well on the layout. A resistance force is also acting on each particle, being proportional to its velocity, in order to relax the system in a final layout. The Barnes-Hut tree algorithm [35] is employed for fast computation, and the Coulomb interaction was calculated on a special-purpose device (GRAPE; gravity pipeline) invented for astrophysical N -body simulation [36]. The result is depicted in Fig. 4. Details of the layout method is given in [37].

One can observe that nodes within a tightly-knit group cluster at mutually near positions in the layout, while different communities are separated from each other with overlapping portions. The sub-communities stated above appear as clusters nested in the community of electronics. Also even closer look in enlargement (not shown in the figure) shows blobs corresponding to hubs or large firms associated with their suppliers and customers.

V. CHAIN OF BANKRUPTCY

Let us now turn our attention to the dynamics on the production network. Firms put value added on intermediate goods in *anticipation* of gaining profits — anticipation, because no firm knows how much their produced goods might actually be demanded by other firms and consumers. In addition, they face uncertainty in the change of costs for intermediate goods to purchase as inputs, as well as in fluctuations of labor and financial costs. Only *a posteriori*, therefore, a firm's profit, being equal to sales minus costs, is determined through the interaction with others in the network.

Supplier-customer link is a credit relation [38]. Whenever one delivers goods to others without an immediate exchange of money or goods of full value, credit is extended. Frequently, suppliers provide credit to their customers, who supply credit to their customers and so forth. Also customers can provide credit to their suppliers so as to have them produce an abundance of intermediate goods beforehand. In either case, once a firm goes into financial insolvency state, its creditors will possibly lose the scheduled payment, or goods to be delivered that have been necessary for production. The influence propagates from the bankrupted customer to its upstream in the former cases, and similarly from the bankrupted supplier to its downstream in the latter cases. Thus a creditor has its balance-sheet deteriorated in accumulation, and may eventually go into bankruptcy. This is an

example of a *chain of bankruptcy*.

A bankruptcy chain does not occur only along the supplier-customer links. Ownership relation among firms is another typical possibility for such creditor-debtor relationship. It is, however, also frequently observed in our dataset that supplier-customer links are also present between holding and held companies, and siblings and affiliated firms. We assume that most relevant paths along which the chain of bankruptcy occurs are the creditor-debtor links of the production network.

As explained in Section II, we have an exhaustive list of bankruptcies. Corresponding to the snapshot of the network taken in September 2006, we employ all the bankruptcies for exactly one-year period from October. The number of bankruptcies amounts to roughly 0.013 million, daily mean being 30, and includes a few bankruptcies of listed firms. Nearly half of the bankrupted firms, precisely $N_b \equiv 6264$, were present on the network at the beginning and went into bankruptcy during the period. The rest are of extremely small-size, typically with one employee, and were not included as nodes, which we assume irrelevant to our purpose as well as new entry of firms during the same period.

Let us define the probability of bankruptcy in the one-year period by the ratio between the number of bankrupted nodes, N_b , and the initially present nodes, N given by (1), by

$$p = N_b/N \approx 0.620\% . \quad (11)$$

Note that the probability has inverse of time in its physical dimension. A year was chosen for the time-scale so that it should be longer than the time-scale for financial activities of firms, typically weeks and months, and be shorter than that for the change of network itself.

A. Avalanche-size distribution

Let us first take a look at how a certain size of chain of bankruptcies actually takes place. Here a chain is defined as a set of bankrupted nodes that are connected by links that are present in the initial network. If nodes are white and black according to survival and bankruptcy during the period, a chain means connected black nodes surrounded by white nodes, and its size refers to the number of black nodes in the chain. Note that a chain is not necessarily a path in the graph, but can be a tree, and may include cycles in it.

Fig. 5 shows the size-distribution of such avalanches by filled squares, which represents the frequency distribution of avalanches with a specific size. The observed values are tabulated in Table IV.

B. Evaluation of accidental chain

Let us then evaluate how a certain size of chain of actual bankruptcies occurs more or less frequently than

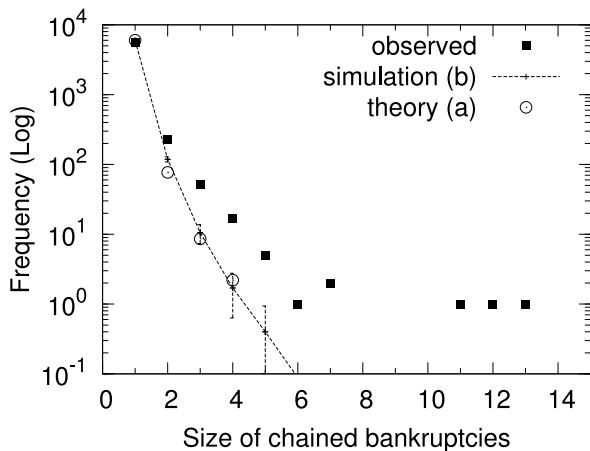


FIG. 5: Frequency (vertical in log-scale) of avalanches with a specific size (horizontal in linear). Filled squares are the observed frequencies in the observation. Open circles show a theoretical calculation for randomized networks with anonymous nodes (see (a) in the text), and a line with error bars represents a Monte-Carlo calculation for randomized networks with same bankrupted nodes as observed ones (b).

TABLE IV: Comparison between the actual value of the chain-bankruptcy and the values expected from coincidence. “Obs.” for the observed values, “Theor.” for the theoretical values of coincidence, “O/T” for the ratios between them, while “RNW” is the value obtained by simulation for the randomized network.

	Obs.	Theor.	O/T	RNW ^a
B_1	5507	6013	0.9	5985(21)
B_2	226	76.9 (82.3 ^b)	2.9	118.5(10.0)
B_3	52	8.6 ^b	6.0	10.5(3.2)
B_4	17	2.2 ^b	7.7	1.7(1.1)

^aStandard deviations in parentheses (each 1,000 randomizations).

^bMean-field approximations.

what is expected simply by chance. Suppose, in a random network with a specified degree sequence, one selects Np nodes for failure, where p is the probability of failure per node. Then calculate the frequency of a certain number of failed nodes that are connected by links, and we can compare the frequency of accidental chain of failures with that for an actual chain of bankruptcies. We shall use the terms, *failures* and *failed nodes*, to mean a set of black nodes that are selected randomly and uniformly over all the nodes, and to distinguish them from the set of actually observed bankruptcies and bankrupted nodes.

The selection of failed nodes can be done in two ways, that is, (a) by choosing uniformly random nodes to fail irrelevantly from the actual data of nodes, or alternatively (b) by specifying exactly the same bankrupted nodes in the actual data, but in otherwise randomized network with the same degree sequence as the real one. These two ways possibly yield different results for our purpose, so let us perform the evaluation in both ways. The evalua-

tion (a) allows us to understand how the accidental chain is related to the network properties, especially degree distribution and correlation, the results of which were given in Section III. On the other hand, we can take into account of difference between failures and bankruptcies in our terminology here. We elaborate the calculation of (a) in the following Section V C. For the calculation of (b), the estimates are obtained by a Monte Carlo simulation generating random networks with failures associated to the actually bankrupted nodes.

We denote by B_m the number of clusters, each with m failed nodes that are connected by links, in average for randomized networks with the same degree distribution $P(k)$ as the actual production network. Since the clustering coefficient is of the same order of magnitude as what is expected by chance, we assume that the network is tree-like. We shall calculate B_m for $m = 1, 2, 3$ and 4 in order.

The results are summarized in Table IV and Fig. 5 for the actually observed values of B_m along with the evaluated values based on the above-mentioned two classes of randomized networks, (a) and (b), in the columns “Theor.” and “RNW” respectively. We find that (a) and (b) give quantitatively similar estimates. By comparing the actually observed values with the evaluation for random networks with a same degree sequence, we can conclude that the avalanche size has a much heavier tail in its distribution for size larger than 3. Those large avalanches involve regionally and industrially related firms, as we could confirm from our dataset. Therefore, the vulnerable paths, along which a chain of bankruptcy takes place are present in those modular groups. The following Section V C is devoted to the explanation of the evaluation (a).

C. Evaluation for accidental chain of failures

We count the number of accidental chain of failures in a given, tree-like network, where all the failures occur randomly with probability p per node.

1. B_1 : Isolated failure

Denoting the number of nodes of degree k by $K_1(k)$, it is related to the degree distribution $P(k)$ by

$$P(k) = \frac{1}{N} K_1(k). \quad (12)$$

Obviously

$$\sum_{k=1}^{\infty} K_1(k) = N. \quad (13)$$

Among $K_1(k)$ such nodes, the average number of failed nodes is $pK_1(k)$. Since the probability that all the nodes

connected to a failed node are not in failure is $(1-p)^k$ (see Fig. 6), the average number of isolated failure is given by

$$B_1 = \sum_{k=1}^{\infty} p K_1(k) (1-p)^k = p N R_1 , \quad (14)$$

$$R_1 \equiv \langle (1-p)^k \rangle , \quad (15)$$

where $\langle \cdot \rangle$ means average over the nodes, *i.e.*,

$$\langle f(k) \rangle \equiv \frac{\sum_{k=1}^{\infty} f(k) K_1(k)}{\sum_{k=1}^{\infty} K_1(k)} . \quad (16)$$

Note that since Np is equal to the actual number of the bankruptcies, R_1 gives the rate of the isolated failure. From the observed distribution of $K_1(k)$ and $p \approx 0.006204$, we obtain

$$R_1 \approx 0.9600 , \quad (17)$$

$$B_1 \approx 6013.2 . \quad (18)$$

The actual number of the *isolated* bankruptcies is 5,507, being 92% of this estimate. Following the standard argument for $1/\sqrt{n}$ estimate of the statistical errors, we see that there are less number of isolated bankruptcies in actuality than that expected by chance.

The results (17) and (18) apply to any class of networks with the same degree sequence $K_1(k)$, in particular, irrespectively of degree correlation.

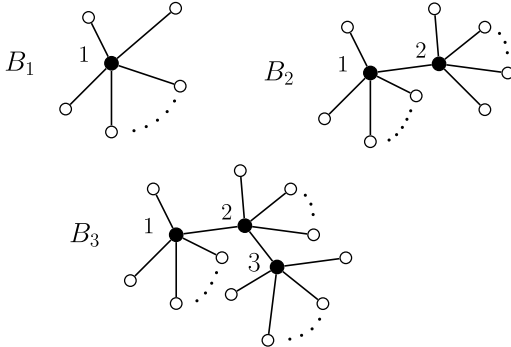


FIG. 6: Clusters of m failed nodes that are connected by links, which contribute to $B_{1,2,3}$. Black nodes are failed ones, and white nodes are non-failed. The numbers attached with failed nodes correspond to the subscripts of degrees, j for k_j .

2. B_2

We denote by $K_2(k_1, k_2)$, the number of pairs of nodes; each pair of nodes having degree k_1 and k_2 . Precisely, choose a node with degree k_1 , and count the nodes with degree k_2 connected with the first node. After doing this

over all the nodes and by adding up the resulting numbers, one has the quantity $K_2(k_1, k_2)$. Now the number of double-failure case, B_2 , can be expressed by $K_2(k_1, k_2)$ as follows:

$$B_2 = \frac{1}{2} \sum_{k_1, k_2=1}^{\infty} K_2(k_1, k_2) p(1-p)^{k_1-1} p(1-p)^{k_2-1} \\ = \frac{1}{2} \frac{p^2}{(1-p)^2} R_2 \sum_{k_1, k_2=1}^{\infty} K_2(k_1, k_2) , \quad (19)$$

$$R_2 \equiv \langle (1-p)^{k_1+k_2} \rangle_2 , \quad (20)$$

where the combinatorial factor $1/2$ accounts for the over-counting the chain in the reverse order of k_1 and k_2 , and $\langle \cdot \rangle_2$ denotes the average over the links, defined by

$$\langle f(k_1, k_2) \rangle_2 \equiv \frac{\sum_{k_1, k_2=1}^{\infty} K_2(k_1, k_2) f(k_1, k_2)}{\sum_{k_1, k_2=1}^{\infty} K_2(k_1, k_2)} . \quad (21)$$

From the definition, $K_2(k_1, k_2)$ satisfies the identities:

$$K_2(k_1, k_2) = K_2(k_2, k_1) , \quad (22)$$

$$\sum_{k_2=1}^{\infty} K_2(k_1, k_2) = k_1 K_1(k_1) . \quad (23)$$

The two identities lead to the summation formula:

$$\sum_{k_1, k_2=1}^{\infty} K_2(k_1, k_2) = N \langle k \rangle , \quad (24)$$

which is exactly twice the number of links, as it should be. The following identity is also useful.

$$\sum_{k_1, k_2=1}^{\infty} K_2(k_1, k_2) k_2^n = N \langle k \rangle \langle k_2^n \rangle_2 = N \langle k^{n+1} \rangle . \quad (25)$$

Using Eq. (24), B_2 can be put as

$$B_2 = \frac{1}{2} \frac{p^2}{(1-p)^2} R_2 N \langle k \rangle . \quad (26)$$

The factor R_2 can be calculated directly from the actual values of $K_2(k_1, k_2)$. The result is

$$R_2 \approx 0.488 , \quad (27)$$

which leads to

$$B_2 \approx 76.9 . \quad (28)$$

The observed value is about three times of this estimate, as shown in Table IV, which indicates the double-failure chain is much more abundant than what is expected by chance.

— Random-network approximation —

In the case of random network, the estimation reduces to a simple expression. In fact, first note that $K_2(k_1, k_2)$ can be written in terms of $K_1(k)$ as follows:

$$K_2^{(\text{ran})}(k_1, k_2) = \frac{1}{N \langle k \rangle} K_1(k_1) k_1 k_2 K_1(k_2) , \quad (29)$$

because it is equal to the number of nodes of degree k_1 , $K_1(k)$, multiplied by the probability of choosing the node of degree k_2 , $k_2 K_1(k_2) / \sum_{k_2=1}^{\infty} k_2 K_1(k_2)$. Note that (29) satisfies the identities (22) and (23) as is required for the consistency of the calculation. Inserting (29) into (20) and (21), the value of R_2 in this approximation is given by

$$R_2^{(\text{ran})} = R_{11}^2 , \quad (30)$$

where

$$R_{11} \equiv \frac{\langle k(1-p)^k \rangle}{\langle k \rangle} \approx 0.723 . \quad (31)$$

This yields

$$R_2^{(\text{ran})} \approx 0.523 , \quad (32)$$

and

$$B_2^{(\text{ran})} = \frac{1}{2} \frac{p^2}{(1-p)^2} R_2^{(\text{ran})} N \langle k \rangle \approx 82.3 , \quad (33)$$

as being tabulated in Table IV.

3. B_3

We define $K_3(k_1, k_2, k_3)$ in a similar way for $K_2(k_1, k_2)$; take a node with degree k_1 , continue the counting to nodes with degree k_2 and then k_3 (see Fig. 6). B_3 is given by

$$\begin{aligned} B_3 &= \frac{1}{2} \sum_{k_1, k_2, k_3=1}^{\infty} K_3(k_1, k_2, k_3) \\ &\quad \times p(1-p)^{k_1-1} p(1-p)^{k_2-2} p(1-p)^{k_3-1} \\ &= \frac{1}{2} \frac{p^3}{(1-p)^4} R_3 K_3^{(\text{sum})} , \end{aligned} \quad (34)$$

$$R_3 \equiv \langle (1-p)^{k_1+k_2+k_3} \rangle_3 , \quad (35)$$

$$K_3^{(\text{sum})} \equiv \sum_{k_1, k_2, k_3=1}^{\infty} K_3(k_1, k_2, k_3) , \quad (36)$$

where the combinatorial factor $1/2$ is to cancel the overcounting, and $\langle \cdot \rangle_3$ refers to the average weighted with $K_3(k_1, k_2, k_3)$ in the same manner as that in Eq. (16) and (21).

By definition, $K_3(k_1, k_2, k_3)$ satisfies the following identities:

$$K_3(k_1, 0, k_3) = 0 , \quad (37)$$

$$K_3(k_1, k_2, k_3) = K_3(k_3, k_2, k_1) , \quad (38)$$

$$\sum_{k_3=1}^{\infty} K_3(k_1, k_2, k_3) = K_2(k_1, k_2)(k_2 - 1) . \quad (39)$$

Using the identities (39) and (23) we find that

$$K_3^{(\text{sum})} = N (\langle k^2 \rangle - \langle k \rangle) \approx 3.09 \times 10^9 . \quad (40)$$

— Random-network approximation —

Since exact evaluation of R_3 involves the evaluation of $K_3(k_1, k_2, k_3)$, which requires a huge computational resource, let us evaluate R_3 by using a random-network approximation. By considering attaching the nodes #2 and #3 successively to the node #1 with equal probability on each links as in the case of $K_2^{(\text{ran})}$, we obtain the following:

$$\begin{aligned} K_3^{(\text{ran})}(k_1, k_2, k_3) &= \\ &= \frac{1}{N^2 \langle k \rangle^2} K_1(k_1) k_1 k_2 K_1(k_2) (k_2 - 1) k_3 K_1(k_3) , \end{aligned} \quad (41)$$

which satisfies identities (37)–(40), except that K_2 is replaced by $K_2^{(\text{ran})}$ in (39). By using the above in (34) we obtain;

$$R_3^{(\text{ran})} = R_{11}^2 \frac{R_{12} \langle k^2 \rangle - R_{11} \langle k \rangle}{\langle k^2 \rangle - \langle k \rangle} \quad (42)$$

where

$$R_{12} \equiv \frac{\langle k^2(1-p)^k \rangle}{\langle k^2 \rangle} \approx 0.0450 . \quad (43)$$

This leads to

$$R_3^{(\text{ran})} \approx 0.0226 , \quad (44)$$

$$B_3^{(\text{ran})} \approx 8.55 . \quad (45)$$

4. B_4

The clusters that contribute to B_4 are illustrated in Fig. 7, and are divided into two types as depicted. One has to understand that larger clusters are more rare events so that statistical errors in observation increase drastically. With this in mind, let us perform estimation, and compare them with the observed values.

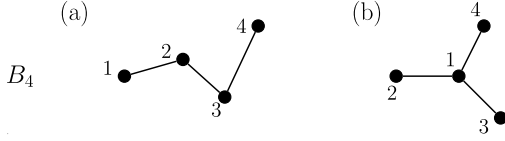


FIG. 7: Two types of clusters that contribute to B_4 . Non-failed nodes (white nodes in Fig. 6) are not drawn.

Type (a)

Contribution of the cluster (a) can be written as follows using the number of strings k_1 - k_4 , $K_4(k_1, k_2, k_3, k_4)$;

$$B_{4a} = \frac{1}{2} p^4 \sum_{k_1, k_2, k_3, k_4=1}^{\infty} K_4(k_1, k_2, k_3, k_4) \times (1-p)^{k_1-1} \left(\prod_{j=2}^3 (1-p)^{k_j-2} \right) (1-p)^{k_4-1} = \frac{1}{2} \frac{p^4}{(1-p)^6} R_{4a} K_4^{(\text{sum})}, \quad (46)$$

$$R_{4a} \equiv \langle (1-p)^{\sum_{i=1}^4 k_i} \rangle_4, \quad (47)$$

where definitions of $\langle \cdot \rangle_4$ and $K_4^{(\text{sum})}$ should be self-evident.

Let us first calculate $K_4^{(\text{sum})}$. The identities satisfied by $K_4(k_1, k_2, k_3, k_4)$ are similar to those of $K_3(k_1, k_2, k_3)$ and would be now obvious. Using them, the summations over k_1 and k_4 can be carried out as follows,

$$K_4^{(\text{sum})} = \sum_{k_2, k_3=1}^{\infty} K_2(k_2, k_3)(k_2-1)(k_3-1) \quad (48)$$

In the expansion of each summand, all the terms except for those of $k_2 k_3$ allow further summation by repeatedly using the identities given so far. On the other hand, since the coefficient of the $k_2 k_3$ -term is $K_2(k_2, k_3)$, this term should be related to degree correlation. As usual, we define the correlation coefficient r_1 by

$$r_1 \equiv \frac{\langle k_1 k_2 \rangle_2 - \langle k_1 \rangle_2^2}{\langle k_1^2 \rangle_2 - \langle k_1 \rangle_2^2}, \quad (49)$$

Using this definition, we can write that

$$\begin{aligned} \langle k_1 k_2 \rangle_2 &= r_1 \langle k^2 \rangle_2 + (1-r_1) \langle k \rangle_2^2 \\ &= r_1 \frac{\langle k^3 \rangle}{\langle k \rangle} + (1-r_1) \left(\frac{\langle k^2 \rangle}{\langle k \rangle} \right)^2, \end{aligned} \quad (50)$$

where we used Eq. (25) and re-labeled the subscripts in the degrees. Thus the $k_2 k_3$ -term reads

$$\begin{aligned} \sum_{k_1, k_2=1}^{\infty} k_1 k_2 K_2(k_1, k_2) &= N \langle k \rangle \langle k_1 k_2 \rangle_2 \\ &= N \left(r_1 \langle k^3 \rangle + (1-r_1) \frac{\langle k^2 \rangle^2}{\langle k \rangle} \right). \end{aligned} \quad (51)$$

Putting all the terms together, we have

$$K_4^{(\text{sum})} = N \left(r_1 \langle k^3 \rangle + (1-r_1) \frac{\langle k^2 \rangle^2}{\langle k \rangle} - 2 \langle k^2 \rangle + \langle k \rangle \right). \quad (52)$$

The random-network approximation for this case requires a careful treatment because of the appearance of the degree correlation coefficient r_1 in the above summation formula. Although its value given in (9) is small, it has a critical role in the above equations: If we use the random-network approximation for K_2 given in (29), we obtain the $r_1 = 0$ result;

$$\sum_{k_1, k_2=1}^{\infty} k_1 k_2 K_2^{(\text{ran})}(k_1, k_2) = N \frac{\langle k^2 \rangle^2}{\langle k \rangle} \approx 1.188 \times 10^{12}, \quad (53)$$

while the exact value is

$$\sum_{k_1, k_2=1}^{\infty} k_1 k_2 K_2(k_1, k_2) \approx 1.342 \times 10^{11}. \quad (54)$$

The role of the correlation coefficient r_1 is evident in these values; it brings in partial cancellations between the first term and the second term, so that the actual value is much smaller than that of the random-network value (53). Note that this is deeply connected with the asymptotic behavior of the degree distribution noted in Section III B: If all the moments of degree is of order one, the effect of the correlation coefficient r_1 is not this drastic. However, due to the degree distribution being power-law, the moments $\langle k^2 \rangle$ and $\langle k^3 \rangle$ are proportional to a positive power of N (we will elaborate on the analysis in Appendix refsec:appA) and thus are quite large, resulting in the importance of cancellation by r_1 observed above.

For this reason, we evaluate B_{4a} in two schemes in the following. The first scheme is to use the exact distribution for $K_2(k_2, k_3)$ but use the random-network approximation for k_1 and k_4 , so that (54) is satisfied. The second one is to use the random-network approximation to all the nodes in K_4 . We will carry out the calculation of both schemes separately.

— Random-network approximation 1 —

The first approximation scheme is given by

$$\begin{aligned} K_4^{(\text{ran1})}(k_1, k_2, k_3, k_4) &= \frac{1}{N^2 \langle k \rangle^2} \\ &\times K_1(k_1) k_1 (k_2-1) K_2(k_2, k_3) (k_3-1) k_4 K_1(k_4), \end{aligned} \quad (55)$$

which is obtained by attaching the #1 and #4 nodes to a #2-#3 pair randomly. It is evident that this satisfies

the identity (48) and therefore (52). It then follows that

$$\begin{aligned} R_{4a}^{(\text{ran1})} &= \frac{R_{11}^2}{K_4^{(\text{sum})}} \\ &\times \sum_{k_2, k_3=1}^{\infty} (1-p)^{k_2+k_3} (k_2-1)(k_3-1) K_2(k_2, k_3) \\ &\approx 8.33 \times 10^{-3} . \end{aligned} \quad (56)$$

From this we obtain

$$B_{4a}^{(\text{ran1})} \approx 0.819 . \quad (57)$$

— Random-network approximation 2 —

In the second, complete random-network approximation, we have

$$\begin{aligned} K_4^{(\text{ran2})}(k_1, k_2, k_3, k_4) &= \frac{1}{N^3 \langle k \rangle^3} \\ &\times K_1(k_1) k_1 k_2 K_1(k_2) (k_2-1) k_3 K_1(k_3) (k_3-1) k_4 K_1(k_4) , \end{aligned} \quad (58)$$

which is obtained by connecting the node #2,3,4 in sequence, or alternatively, by substituting the random network approximation $K_2^{(\text{ran})}$ in (29) for K_2 in (55). We then obtain the following:

$$\begin{aligned} R_{4a}^{(\text{ran2})} &= R_{11}^2 \left(\frac{R_{12} \langle k^2 \rangle - R_{11} \langle k \rangle}{\langle k^2 \rangle - \langle k \rangle} \right)^2 \\ &\approx 9.77 \times 10^{-4} , \end{aligned} \quad (59)$$

which leads to

$$B_{4a}^{(\text{ran2})} \approx 0.884 , \quad (60)$$

which is very close to $B_{4a}^{(\text{ran1})}$.

Type (b)

For the other type of (b), we can write as

$$\begin{aligned} B_{4b} &= \frac{1}{3!} p^4 \sum_{k_1, k_2, k_3, k_4=1}^{\infty} J_4(k_1, k_2, k_3, k_4) \\ &\times (1-p)^{k_1-3} \prod_{j=2}^4 (1-p)^{k_j-1} \\ &\equiv \frac{1}{3!} \frac{p^4}{(1-p)^7} R_{4b} J_4^{(\text{sum})} , \end{aligned} \quad (61)$$

where

$$J_4^{(\text{sum})} \equiv \sum_{k_1, k_2, k_3, k_4=1}^{\infty} J_4(k_1, k_2, k_3, k_4) , \quad (62)$$

and R_{4b} is a ratio defined by the above. In this case, we denote by $J_4(k_1, k_2, k_3, k_4)$, the number of the clusters of

type (b) with the degrees k_i of nodes # i in Fig. 7. The combinatorial factor $1/3!$ cancels the over-counting of a same cluster. The following identities hold:

$$J_4(k_1, k_2, k_3, k_4) = J_4(k_1, k_{\sigma(2)}, k_{\sigma(3)}, k_{\sigma(4)}) , \quad (63)$$

$$\sum_{k_4=1}^{\infty} J_4(k_1, k_2, k_3, k_4) = K_3(k_2, k_1, k_3) (k_1-2) , \quad (64)$$

where $\sigma(j)$ represents a permutation of $j = 2, 3, 4$. Using the identities, we have

$$\sum_{k_3, k_4=1}^{\infty} J_4(k_1, k_2, k_3, k_4) = K_2(k_2, k_1) (k_1-1) (k_1-2) , \quad (65)$$

which leads to

$$J_4^{(\text{sum})} = N (\langle k^3 \rangle - 3 \langle k^2 \rangle + 2 \langle k \rangle) . \quad (66)$$

— Random-network approximation —

As seen in (66), the degree-correlation does not play any major role for this type of cluster. So, unlike the case of B_{4a} , let us employ a simple random-network approximation of the form:

$$\begin{aligned} J_4^{(\text{ran})}(k_1, k_2, k_3, k_4) &= \frac{1}{N^3 \langle k \rangle^3} K_1(k_1) \\ &\times k_1 k_2 K_1(k_2) (k_1-1) k_3 K_1(k_3) (k_1-2) k_4 K_1(k_4) , \end{aligned} \quad (67)$$

which satisfies identities (63)–(66) with K_2 replaced by $K_2^{(\text{ran})}$. We obtain the following:

$$\begin{aligned} R_{4b}^{(\text{ran})} &= R_{11}^3 \frac{R_{13} \langle k^3 \rangle - 3R_{12} \langle k^2 \rangle + R_{11} \langle k \rangle}{\langle k^3 \rangle - 3 \langle k^2 \rangle + \langle k \rangle} \\ &\approx 3.52 \times 10^{-4} , \end{aligned} \quad (68)$$

where

$$R_{13} \equiv \frac{\langle k^3 (1-p)^k \rangle}{\langle k^3 \rangle} \approx 9.57 \times 10^{-4} . \quad (69)$$

This leads to

$$B_{4b}^{(\text{ran})} \approx 1.39 . \quad (70)$$

VI. DISCUSSION

In the preceding section, we found that the size of chained bankruptcies is frequently larger than what is expected simply by chance. This fact implies that supplier-customer links can be potentially a vulnerable path for a chain of bankruptcies causing a sequence of failures, and that it is important to do monitoring and prediction of such failures on a nation-wide scale. Let us remark a few things concerning the finding.

Firstly, the study on community structure in Section IV showed that the firms are often tightly knitted into clusters characterized by closeness in industrial sectors and/or geographical locations. Because those firms in such a cluster are susceptible to common risk factors specific to the sector or the location, the bankruptcies in a cluster can be correlated due to the similar profiles of those firms, but not necessarily due to the “link” effect.

It is not easy, in the present analysis, to separate the link effect from the sectoral or locational correlation, but yet we can roughly estimate the relative importance of the link effect. Although it is difficult to determine a single cause in each bankruptcy, there exists a pattern of types in the cause of failure, which are categorized and compiled in the database. The most frequent one is the poor performance in business, typically slow sales and decreasing profit due to adverse and sluggish market conditions. The other main category is the linked failure due to a secondary effect from bankruptcy of customer, subsidiary or affiliated companies, which often causes the loss of accounts receivable. See [39] for the details.

For the bankrupted nodes N_b studied in Section V, the categorized causes of bankruptcy are the poor performance (60%) and the link effect (7%). But if a pair of bankrupted nodes are connected by a supplier-customer link, the link effect is considerable (27%), while the poor performance cases or “solo” failures are relatively less frequent (42%). This fact, therefore, shows that the chain of bankruptcy we observed in the preceding section is largely, even if not entirely, due to the link effect taking place along the supplier-customer links.

Secondly, the chain of bankruptcy has a great influence in a nation-wide economy. In fact, the total amount of debts for bankrupted firms in a year typically ranges from 10 to 25 trillion yen in the last 10 years, roughly equal to more than 100 billion euro. This amounts to 2% or even more of the nominal GDP in Japan. Of course, all the debts are not to be lost, but it should not be undervalued the fact that there are a large number of creditors who have given credits to those bankrupted firms. Therefore, the study on the chain of failures and its ripple effect has practical applications. Recent models such as a model of credit chains and bankruptcies [9], simulation of avalanche effect [40], Potts-like model of contagion [11] (see also references in [18]) would provide valuable insights and tools to do monitoring of financial fragility and prediction of such failures on a nation-wide scale.

Thirdly, from a broader perspective, the production

network has a similarity in its structure with other economic networks. While the inter-bank networks have unique structure among financial institutions [12–14], and the banks-firms networks is basically a bipartite network [15], the ownership networks [16, 17] possess similar properties of network. In particular, the community structure has industry-sectoral modules in a hierarchical way. However, the common sets of supplies play important constituents in the production network, as we have explained by the example of automobile companies in Section IV, and this is completely different from the ownership networks. We would yet need a more systematic comparison with other economic networks for the study of similarity and dissimilarity.

VII. SUMMARY

We studied a large-scale structure of the nation-wide production network comprising a million firms and four million supplier-customer links in Japan. The set of nodes covers most active firms. Each link was chosen and considered as important, in a systematic survey of credit informations, by at least one of the firms at either end of the link, as its suppliers and customers. We found scale-free degree distribution, disassortativity, correlation of degree to firm-size, and small clustering coefficients compared with randomized networks with the same degree sequence. In the community analysis, which is based on modularity optimization, we were able to identify communities in the manufacturing sector, and found that they can be interpreted as modules depending on industrial sectors and geographical regions. Large communities contained subgroups that can be characterized also by industrial organization and development.

In addition, by employing an exhaustive list of bankruptcies that took place on the production network, we took a close look at the size distribution for chains of bankruptcies, or avalanche-size distribution. We elaborated a method to evaluate the frequencies of accidental chain in randomized networks, and found that the actual avalanche has a heavy tail distribution in its size. Combining with the large-scale properties and heterogeneity in modular structures, we claim that the effect to a number of creditors, non-trivially large due to the heavy tail in the degree distribution, is considerable in the real economy of the nation.

Acknowledgments

We would like to thank Tokyo Shoko Research, Ltd. in Japan for kindly providing us with a chance to study their large datasets for the academic purpose. Network analysis was partially carried out on Altix3700 at YITP in Kyoto University. Y. F. thanks Y. I. Leon Suematsu for an implementation of fast community extraction, Y. Fujita and A. Kawai for a large-graph layout by GRAPE (grav-

ity pipe). We would like to thank Y. Ikeda, H. Iyetomi, J. Kertész, M. Gallegati, W. Souma for useful comments and additional references.

Appendix A: Analytic estimates of R 's and the asymptotic behavior of the degree distribution

Since the probability of failure p is small, one might want to utilize a perturbative evaluation of the ratios, R 's. Indeed such an analytical expression would be helpful in understanding what essentially determines the rate of the chain-bankruptcy. In this Appendix, we show that the asymptotic behavior of the degree distribution plays the key role.

Let us denote the probability density function (pdf) of the degree k by $P(k)$ and its cumulative distribution function (cdf) by

$$P_{>}(k) = \sum_{k'=k}^{\infty} P(k'). \quad (\text{A1})$$

We parametrize the cdf as

$$P_{>}(k) \sim \left(\frac{k}{k_0}\right)^{-\mu}, \quad (\text{A2})$$

for large k . It follows that $P(k) \propto k^{-\mu-1}$ in the same region. For our data of the production network regarded as an undirected graph, we have

$$\mu \approx 1.366, \quad (\text{A3})$$

$$k_0 \approx 2.18, \quad (\text{A4})$$

as maximum likelihood estimate (with the standard error of μ being 0.099).

We define the generating function for the degree distribution by

$$G(q) = \sum_{k=1}^{\infty} e^{-qk} P(k), \quad (\text{A5})$$

which satisfy $G(0) = 1$. The desired ratios are expressed in terms of the generating function $G(q)$ as

$$R_1 = \frac{G(q_0)}{\langle k \rangle},$$

$$R_{1n} = -\frac{G^{(n)}(q_0)}{\langle k^n \rangle},$$

where $G^{(n)}(q)$ is the n -th derivative of $G(q)$ with respect to q , and $q_0 = -\log(1-p) \approx 6.20 \times 10^{-3}$.

One might attempt the following analytic expansion of $G(q)$:

$$G(q) = \sum_{k=1}^{\infty} \left(1 - qk + \frac{1}{2}q^2k^2 + \dots\right) P(k)$$

$$= 1 - \langle k \rangle q + \frac{1}{2} \langle k^2 \rangle q^2 + \dots \quad (\text{A6})$$

This turns out to be *not* a useful expansion as is shown in what follows. Instead, we shall give an improved expansion.

For the distribution (A2), the second moment of degree is divergent for $\mu < 2$ in a network with an infinite size. It is finite but has a large value for network of a finite size. Actually, for our data

$$\langle k^2 \rangle = 3069.6, \quad (\text{A7})$$

while $\langle k \rangle = 8.006$. So the expansion to the second order is a good approximation only for

$$q \ll \frac{\langle k \rangle}{\langle k^2 \rangle} \approx 2.61 \times 10^{-3}, \quad (\text{A8})$$

but this does not hold in the present case. This is illustrated in Fig. 8, where the solid curve is the actual $G(q)$, the curve (a) the first two terms in the expansion (A6), the curve (b) all three terms in the expansion (A6).

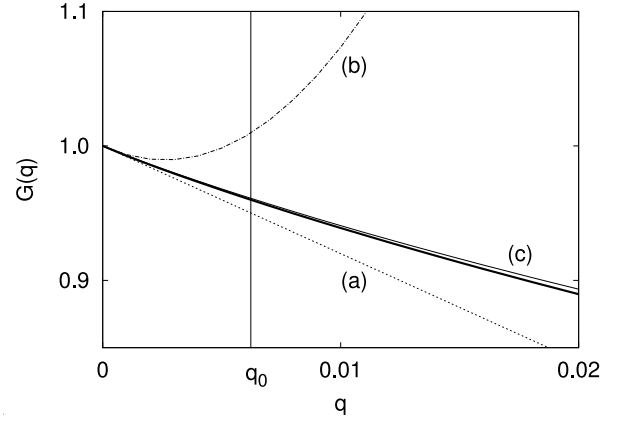


FIG. 8: The generating function for the degree distribution, $G(q)$ for $q \approx 0$. The solid curve is the actual plot. The first-order and the second-order approximations in Eq. (A6) are shown by the dashed line (a) and the dash-dot line (b) respectively. The dotted line (c) is the improved expansion given by (A15). The vertical line corresponds to the actual value of $q_0 = -\log(1-p)$.

Let us now estimate the order of the coefficients of the naive expansion (A6) analytically. The m -th moment of degree is dominated by the large k region for $m > \mu$ as

$$\langle k^m \rangle \propto \sum_{k=1}^{k(\max)} k^m k^{-\mu-1}$$

$$\simeq \int_{k(\max)}^{\infty} k^m k^{-\mu-1} dk \simeq k_{(\max)}^{m-\mu}. \quad (\text{A9})$$

On the other hand, by considering the node of the largest degree being the top of the cdf (A2), we have

$$k_{(\max)}^{-\mu} \propto \frac{1}{N}. \quad (\text{A10})$$

Therefore, we obtain

$$\langle k^m \rangle \propto N^{-1+\frac{m}{\mu}}, \quad (\text{A11})$$

TABLE V: The true values and the estimates obtained from (A15).

Ratio	Exact value	Estimate	Difference
R_1	0.9600	0.9611	0.11%
R_{11}	0.7230	0.7017	-2.9%
R_{12}	4.501×10^{-2}	4.575×10^{-2}	1.6%
R_{13}	9.574×10^{-4}	9.440×10^{-4}	-1.3%

for $m > \mu$. It follows from (A11) that the m -th term in (A6) is of order,

$$\frac{N^{-1}}{m!} \left(N^{1/\mu} q \right)^m. \quad (\text{A12})$$

Therefore the m -th order term is of the same order of magnitude as the $(m+1)$ -th order term provided that

$$m \simeq N^{1/\mu} q \approx 154.7, \quad (\text{A13})$$

meaning that we need much more than 155 terms for the expansion (A6) to be useful for evaluation of our ratios.

An improved approximation can be obtained as follows. Let us extract an analytic contribution of the

power-law tail by means of an analytic continuation:

$$\int_0^\infty \mu \frac{k^{-\mu-1}}{k_0^{-\mu}} e^{-qk} dk \simeq \mu (qk_0)^\mu \Gamma(-\mu). \quad (\text{A14})$$

For $1 < \mu < 2$, this contribution is of larger power of p than that of the second-order, p^2 , term in (A6). Therefore, we arrive at the following approximation,

$$G(q) = 1 - \langle k \rangle q + \mu \Gamma(-\mu) (k_0 q)^\mu + \dots. \quad (\text{A15})$$

Alternatively, this expression can be obtained by evaluating the dominant $k \sim k_{(\max)}$ contribution in $G(q) - (1 - \langle k \rangle q)$. Also it should be noted that this expression is valid for $q \gg 1/k_{(\max)}$, since we extended the integration to $k = \infty$ in (A14), instead of cutting it off at $k = k_{(\max)}$. The curve (c) in Fig. 8 depicts the behavior of the first three terms on the right-hand side of (A15). It is evident that the improved expansion works as an excellent approximation as shown in the plot. In fact, the comparison between the estimates of the ratios obtained from (A15) and the true values are excellent as seen in Table. V.

-
- [1] R. Albert and A.-L. Barabási. Statistical mechanics of complex networks. *Reviews of Modern Physics*, 74(1):47–97, 2002.
- [2] S. N. Dorogovtsev and J. F. F. Mendes. Evolution of networks. *Advances in Physics*, 51(4):1079–1187, 2002.
- [3] M. E. J. Newman. The structure and function of complex networks. *SIAM Review*, 45(2):167–256, 2003.
- [4] P. Bak, K. Chen, J. A. Scheinkman, and M. Woodford. Aggregate fluctuations from independent sectoral shocks. *Ricerche Economiche*, 47:3–30, 1993.
- [5] J. A. Scheinkman and M. Woodford. Self-Organized Criticality and Economic Fluctuations. *The American Economic Review*, 84(2):417–421, 1994.
- [6] M. Nirei. (S,s) inventory dynamics and self-organized criticality. *Research in Economics*, 54:375–383, 2000.
- [7] P. Bak. *How Nature Works*. Springer-Verlag, 1996.
- [8] G. Weisbuch and S. Battiston. Production networks and failure avalanches. *Journal of Economic Behavior & Organization*, 64:448–469, 2007.
- [9] S. Battiston, D. Delli Gatti, M. Gallegati, B. Greenwald, and J. E. Stiglitz. Credit chains and bankruptcies propagation in production networks. *Journal of Economic Dynamics & Control*, 31:2061–2084, 2007.
- [10] J. Lorenz and S. Battiston. Systemic risk in a network fragility model analyzed with probability density evolution of persistent random walks. *Network and Heterogeneous Media*, 3(2):185–200, 2008.
- [11] P. Sieczka and J. A. Holyst. Collective firm bankruptcies and phase transition in rating dynamics. *European Physical Journal B*, 71:461–466, 2007.
- [12] G. De Masi, G. Iori, and G. Caldarelli. Fitness model for the Italian interbank money market. *Physical Review E*, 74:066112, 2006.
- [13] G. Iori, G. De Masi, O. V. Precup, G. Gabbi, and G. Caldarelli. A Network Analysis of the Italian Overnight Money Market. *Journal of Economics Dynamics and Control*, 32:259–278, 2008.
- [14] F. Kyriakopoulos, S. Thurner, C. Pühr, and S. W. Schmitz. Network and eigenvalue analysis of financial transaction networks. *European Physical Journal B*, 71:523–531, 2009.
- [15] G. De Masi, Y. Fujiwara, M. Gallegati, B. Greenwald, and J. E. Stiglitz. An analysis of the Japanese credit network. arXiv:0901.2384v1 [q-fin.ST].
- [16] D. Garlaschelli and M. I. Loffredo. Structure and evolution of the world trade network. *Physica A*, 355:138–144, 2005.
- [17] J. B. Glattfelder and S. Battiston. Backbone of complex networks of corporations: The flow of control. *Physical Review E*, 80:036104, 2009.
- [18] F. Schweitzer, G. Fagiolo, D. Sornette, F. Vega-Redondo, and D. White. Economic Networks: What do we know and what do we need to know? *Advances in Complex Systems*, 12:407–422, 2009.
- [19] Y. U. Saito, T. Watanabe, and M. Iwamura. Do larger firms have more interfirm relationships? *Physica A*, 383(1):158–163, 2007.
- [20] T. Ohnishi, H. Takayasu, and M. Takayasu. Hubs and Authorities on Japanese Inter-Firm Network: Characterization of Nodes in Very Large Directed Networks. *Progress of Theoretical Physics Supplement*, (179):157–167, 2009.
- [21] A. Broder, R. Kumar, F. Maghoul, P. Raghavan, S. Rajagopalan, A. Stata, R. and Tomkins, and J. Wiener. Graph structure in the Web. *Computer Networks*, 33(1-6):309–320, 2000.

- [22] B.M. Hill. A Simple General Approach to Inference About the Tail of a Distribution. *The Annals of Statistics*, 3(5):1163–1174, 1975.
- [23] W. H. Press, S. A. Teukolsky, W. T. Vetterling, and B. P. Flannery. *Numerical Recipes in C: The Art of Scientific Computing*. University of Cambridge, second edition, 1992.
- [24] M. E. J. Newman. *Random graphs as models of networks*, chapter 2, pages 35–68. Wiley-VCH Weinheim, 2003. in ed. S. Bornholdt and H. G. Schuster, Handbook of graphs and networks.
- [25] M. E. J. Newman. Mixing patterns in networks. *Physical Review E*, 67(2):026126, 2003.
- [26] M. E. J. Newman and M. Girvan. Finding and evaluating community structure in networks. *Physical Review E*, 69(2):026113, 2004.
- [27] A. Clauset, M. E. J. Newman, and C. Moore. Finding community structure in very large networks. *Physical Review E*, 70(6):066111, 2004.
- [28] L. Danon, A. Díaz-Guilera, J. Duch, and A. Arenas. Comparing community structure identification. *Journal of Statistical Mechanics*, 2005(09):P09008, 2005.
- [29] S. Fortunato and M. Barthelemy. Resolution limit in community detection. *Proceedings of the National Academy of Sciences*, 104(1):36–41, 2007.
- [30] J. M. Kumpula, J. Saramäki, K. Kaski, and J. Kertész. Limited resolution in complex network community detection with Potts model approach. *European Physical Journal B*, 56(1):41–45, 2007.
- [31] Kumpula, J. M. and Saramäki, J. and Kaski, K. and Kertész, J. Limited resolution and multiresolution methods in complex network community detection. *Fluctuation and Noise Letters*, 7(3):L209–L214, 2007.
- [32] Lancichinetti, A. and Fortunato, S. and Kertész, J. Detecting the overlapping and hierarchical community structure of complex networks. *New J. Phys.*, 11:033015, 2009.
- [33] M. Sales-Pardo, R. Guimera, A. A. Moreira, and L. A. N. Amaral. Extracting the hierarchical organization of complex systems. *Proceedings of the National Academy of Sciences*, 104(39):15224–15229, 2007.
- [34] A. Clauset, C. Moore, and M. E. J. Newman. Hierarchical structure and the prediction of missing links in networks. *Nature*, 453(7191):98–101, 2008.
- [35] J. Barnes and P. Hut. A hierarchical $O(N \log N)$ force-calculation algorithm. *Nature*, 324(6096):446–449, 1986.
- [36] J. Makino and M. Taiji. *Scientific Simulations with Special-Purpose Computers*. John Wiley and Sons, Chichester, UK, 1998.
- [37] Y. Fujiwara. Visualizing a large-scale structure of production network by N-body simulation. *Progress of Theoretical Physics Supplement*, (179):167–177, 2009.
- [38] J. Stiglitz and B. Greenwald. *Towards a New Paradigm in Monetary Economics*. Cambridge University Press, 2003.
- [39] Y. Fujiwara. Chain of firms bankruptcy: a macroscopic study of link effect in a production network. *Advances in Complex Systems*, 11(5):703–717, 2008.
- [40] Lublóy, Á. and Szenes, M. Network of corporate clients: Customer attrition at commercial banks. *J. Stat. Mech.*, page P12014, 2008.